# METTL5 reprograms glycolytic metabolism and promotes non-small cell lung cancer progression by modifying PGAM1

YUCHEN SHAN[1*], XIAOYU DUAN[1*], KAI YUAN[1,2], MING LOU[1,2], QIYONG WU[1,2] and ZHAOJIA GAO[1,2]

[1]Department of Thoracic Surgery, Changzhou No. 2 People's Hospital (The Third Affiliated Hospital of Nanjing Medical University), Changzhou, Jiangsu 213003, P.R. China; [2]Laboratory of Heart and Lung Disease, Changzhou No. 2 People's Hospital (The Third Affiliated Hospital of Nanjing Medical University), Changzhou, Jiangsu 213003, P.R. China

Received September 19, 2025; Accepted March 4, 2026

DOI: 10.3892/ol.2026.15609

**Abstract.** $N^6$-methyladenosine ($m^6A$) RNA methylation is implicated in cancer metabolism; however, to the best of our knowledge, the role of methyltransferase 5 (METTL5) in non-small cell lung cancer (NSCLC) progression remains unclear. Reprogrammed glycolytic metabolism (Warburg effect) supports tumor growth and immune evasion; however, the regulatory mechanisms of this process require further investigation. We hypothesized that METTL5 drives NSCLC progression by regulating glycolytic metabolism through $m^6A$ modification of phosphoglycerate mutase 1 (PGAM1) mRNA. The present study aimed to elucidate the molecular mechanisms, functional impacts and clinical relevance of the METTL5/PGAM1 axis. Integrated analyses of NSCLC cohorts from The Cancer Genome Atlas database were performed, and *in vitro* models (A549 and PC9 cell lines) and molecular techniques, including methylation inhibition, RNA stability assays and metabolic flux measurements (Seahorse XFe96 analyzer), were used. Key interactions were validated through western blotting, reverse transcription-quantitative PCR and correlation analyses. METTL5 was significantly upregulated in NSCLC tissues and in A549, PC9 and H520 cell lines, and high METTL5 expression was associated with poor patient survival ($P<0.05$). Silencing of METTL5 suppressed NSCLC cell proliferation and migration, while overexpression promoted proliferation and migration. METTL5 directly targeted PGAM1 mRNA through $m^6A$ modification, and the expression levels of METTL5 and PGAM1 exhibited a statistically significant but moderate positive correlation ($R=0.45$; $P=5.4x10^{-56}$). YTH $N^6$-methyladenosine RNA binding protein 1 (YTHDF1) is an m6A reader that recognizes and binds to methylated PGAM1 mRNA, enhancing its stability and expression. PGAM1 knockdown reduced glycolysis (decreased extracellular acidification rate) and increased oxidative phosphorylation (increased oxygen consumption rate). Notably, the positive correlation between PGAM1 and GLUT1 expression ($R=0.6$; $P=4.12x10^{-183}$) supports the role of the METTL5/PGAM1 axis in regulating GLUT1, thereby influencing glycolytic flux. Rescue experiments demonstrated that PGAM1 overexpression reversed GLUT1 downregulation in METTL5-knockdown cells. Overall, METTL5 may drive NSCLC progression by reprogramming glycolytic metabolism through $m^6A$ modification of PGAM1 mRNA. The METTL5/PGAM1/GLUT1 axis represents a novel therapeutic target for NSCLC.

## Introduction

Lung cancer remains a life-threatening malignancy worldwide, with >2 million new cases and ~1.76 million mortalities reported annually (1). Non-small cell lung cancer (NSCLC) is the most predominant subtype, accounting for 85% of all annual lung cancer diagnoses (2). Despite advancements in surgical techniques, precision treatment approaches and immunotherapeutic interventions, the 5-year survival rate of patients with NSCLC has exhibited limited improvement (3,4). Therefore, it is necessary to identify novel biomarkers and develop targeted pharmacological interventions to improve the prognosis of NSCLC (5,6).

A defining characteristic of malignant tumors is reprogrammed energy metabolism, which facilitates tumor development and progression. However, the precise underlying molecular mechanisms warrant further investigation (7,8). The Warburg effect, characterized by enhanced lactate production instead of mitochondrial oxidation under oxygen-rich conditions, represents a fundamental metabolic adaptation in cancer (9,10). This glycolytic pathway serves a dual purpose, as it immediately generates energy substrates while producing key biosynthetic precursors, such as glucose-6-phosphate, pyruvate derivatives and lactate, for macromolecule synthesis. Notably, the lactate accumulated in the tumor

*Correspondence to:* Dr Zhaojia Gao, Department of Thoracic Surgery, Changzhou No. 2 People's Hospital (The Third Affiliated Hospital of Nanjing Medical University), 68 Gehu Middle Road, Changzhou, Jiangsu 213003, P.R. China
E-mail: sweetyfy@live.cn

*Contributed equally

*Key words:* non-small cell lung cancer, $N^6$-methyladenosine RNA methylation, Warburg effect, methyltransferase 5, phosphoglycerate mutase 1, glucose transporter type 1

microenvironment induces extracellular acidification, creating favorable conditions for the metastatic spread and immune evasion of tumor cells (11-13). Studies have shown that lactate can impair immune cell function. In particular, it can suppress the cytotoxic function of natural killer cells and T lymphocytes, facilitating tumor immune evasion by impairing immune surveillance mechanisms (14-16). In addition, lactate can promote the proliferation and differentiation of regulatory T cells, inhibiting antitumor immune responses (17). A number of studies have shown that targeting the glycolytic pathway in cancer cells is a promising therapeutic strategy. For example, phosphoglycerate mutase 1 (PGAM1), a key glycolytic enzyme, has emerged as a key therapeutic target for cancer, and marked advancements have been made in designing PGAM1 inhibitors (18,19).

$N^6$-methyladenosine ($m^6A$) modification, characterized by the addition of a methyl group to the sixth nitrogen of adenine in RNA molecules, is a prevalent post-transcriptional modification in eukaryotic organisms (20,21). This dynamic modification influences the stability, localization and translational efficiency of RNA through enzymatic regulation. $m^6A$ modification is a reversible process regulated by three functional protein groups, namely methyltransferases (writers), demethylases (erasers) and methyl recognition proteins (readers). The methyltransferase complex involved in $m^6A$ modification is composed of core catalytic subunits such as methyltransferase (METTL)-3, METTL5 and Wilms' tumor 1-associating protein (WTAP) and auxiliary components such as vir-like M6A methyltransferase associated (VIRMA), RNA binding motif protein 15 (RBM15) and METTL16 (22-24). Fat mass and obesity-associated protein and α-ketoglutarate-dependent dioxygenase homolog 5 function as key $m^6A$ erasers (demethylases) by catalyzing the removal of methyl groups from modified nucleotides (25,26). YTH protein family members, including YTH $N^6$-methyladenosine RNA binding protein (YTHD)-F1, YTHDF2 and YTHDC2, serve as primary $m^6A$ readers that modulate RNA stability and translational efficiency through selective binding to methylated transcripts (27-29).

$m^6A$ modification serves as an important regulatory mechanism in cancer initiation and progression. In gastric cancer, this epigenetic modification accelerates malignant progression by stimulating key oncogenic pathways, such as the Wnt and PI3K/AKT/mTOR pathways (30-32). METTL3 knockout can markedly inhibit the proliferation and migration of oxaliplatin-resistant gastric cancer cells and induce their apoptosis, thereby enhancing oxaliplatin sensitivity. These findings indicate that $m^6A$ modification may affect chemotherapy resistance in gastric cancer (33). Therefore, small-molecule inhibitors targeting $m^6A$ modification-related enzymes are promising therapeutic agents for cancer (34).

METTL5 is an emerging RNA methyltransferase that catalyzes $m^6A$ modification of target mRNAs, often in complex with regulatory proteins such as WTAP (35). Dysregulation of METTL5 has been associated with tumorigenesis across numerous cancer types, highlighting its context-dependent oncogenic roles. For example, in liver hepatocellular carcinoma (LIHC), the upregulation of METTL5 enhances the stability of c-Myc, which in turn activates glycolytic genes, leading to abnormal glucose metabolism and tumor growth (36). In renal clear cell carcinoma (KIRC), METTL5 participates in regulation of the tumor immune microenvironment and may promote tumor progression by facilitating the infiltration of immunosuppressive cells (37). High METTL5 expression has been shown to be negatively associated with the prognosis of patients with stomach adenocarcinoma. The mechanism involves increased stability of nuclear factor (erythroid-derived 2)-like 2 mRNA, inhibition of $Fe^{2+}$ accumulation and ferroptosis and therefore, suppression of the antitumor immunity mediated by peripheral blood mononuclear cells (38). However, the functional roles and regulatory mechanisms of METTL5 in NSCLC remain poorly understood. In addition, to the best of our knowledge, the mechanisms by which METTL5-mediated $m^6A$ methylation regulates PGAM1 mRNA expression in NSCLC remain unexplored. The potential interplay among METTL5, PGAM1 and glucose transporter type 1 (GLUT1), another key protein in metabolic adaptation (39,40), has not been elucidated. Notably, to the best of our knowledge, the clinical relevance of this regulatory axis and its impact on patient prognosis remain unexplored.

Given these gaps, the present study aimed to determine whether METTL5 is expressed in NSCLC and assess its prognostic importance, investigate the functional role of METTL5 in regulating glycolytic metabolism and tumor progression, elucidate the molecular mechanism by which METTL5 modulates PGAM1 expression through $m^6A$ modification, and examine the downstream effects on GLUT1 expression and metabolic reprogramming. The present investigation of this regulatory axis is considered to provide novel insights for the development of precision therapeutic strategies for NSCLC.

## Materials and methods

*Cell culture and cell lines*. The A549 human lung adenocarcinoma (LUAD) cell line, as well as the BEAS-2B bronchial epithelial cell line, the PC9 LUAD cell line, the H520 lung squamous cell carcinoma cell line and the NCI-H1299 NSCLC cell line were obtained from ZFdows Biotech Co., Ltd. All cell lines were authenticated through short tandem repeat profiling, which determined the absence of *Mycoplasma* contamination. Detailed specifications of all cell lines are provided in Table I, with data derived from the Catalogue of Somatic Mutations in Cancer (Sanger Institute; https://cancer.sanger.ac.uk/cosmic) and the Cancer Cell Line Encyclopedia (American Type Culture Collection; https://www.atcc.org/) databases. All cells were cultured in DMEM/F12 (1:1 ratio; cat. no. BL1917A; Biosharp Life Sciences) enriched with 10% FBS (cat. no. BL305A; Biosharp Life Sciences) under standard conditions (37˚C; 5% $CO_2$) for optimal cell proliferation.

*Cell transfection*. METTL5- and PGAM1-overexpression plasmids were purchased from Heyuan Liji (Shanghai) Biotechnology Co., Ltd. The open reading frames of METTL5 and PGAM1 were cloned into the pcDNA3.1(+) vector. Specific small interfering RNAs (siRNAs), along with a non-targeting negative control siRNA, were obtained from Guangzhou RiboBio Co., Ltd. For transient transfection, cells were seeded in 6-well plates at a density of $3x10^5$ cells per well 24 h prior to transfection. Plasmid DNA (2 $\mu$g) or siRNA (50 nM) were transfected into cells using Lipo8000™ reagent (cat. no. C0533; Beyotime Biotechnology) according

Table I. Cell line characteristics.

| Cell line | Histologic origin | Key driver mutation(s) (COSMIC/ATCC) | TP53 status | Other recurrent alterations | Doubling time, h | Tumorigenicity in mice | Typical applications |
|---|---|---|---|---|---|---|---|
| A549 | Adenocarcinoma (peripheral) | KRAS G12S | Wild-type | STK11 loss, KEAP1 mutation | 22-24 | ++ (s.c. and orthotopic) | KRAS-mutant model; chemo-/radio-/immuno-therapy studies |
| H1299 | Large-cell carcinoma | None (EGFR/KRAS/ALK WT) | Homozygous deletion | NF1 loss, PTEN loss | 20-22 | ++ | p53-null background; high transfection efficiency; gene-rescue assays |
| PC9 | Adenocarcinoma | EGFR E746_A750 deletion (exon 19) | Wild-type | BIM deletion (subset) | 24-26 | ++ | Prototype EGFR/TKI-sensitive line; parental strain for resistant clones |
| H520 | Squamous-cell carcinoma | KRAS G12C + BRAF G466V | Mutant | - | 28-32 | + | Squamous KRAS model; immune-checkpoint studies |
| BEAS-2B | Immortalized (non-cancerous) bronchial epithelium | None | Wild-type | SV40 large T-antigen | 30-34 | - | Normal control for transformation studies; chemical- or oncogene-induced carcinogenesis models; MSC-like properties reported |

COSMIC, Catalogue Of Somatic Mutations In Cancer; ATCC, American Type Culture Collection; s.c., subcutaneous; TKI, tyrosine kinase inhibitor; SV40; simian virus 40; STK11, serine/threonine kinase 11; KEAP1, Kelch-like ECH-associated protein 1; ALK, anaplastic lymphoma kinase; WT, wild-type; MSC, mesenchymal stem cell; BIM, B-cell chronic lymphocytic leukemia-lymphoma like 11 gene; NF1, neurofibromin 1. Tumorigenicity grading: +, low tumorigenic potential or slower tumor formation; ++, high tumorigenic potential or rapid tumor formation in immunodeficient mice.

to the manufacturer's protocol. The transfection mixture was incubated with cells for 6 h at 37˚C before replacing with fresh complete medium. After 48 h transfection, cell samples were collected for protein quantification.

For stable gene knockdown, short hairpin RNA (shRNA/sh)-YTHDF1 and sh-PGAM1 lentiviral particles were obtained from Guangzhou RiboBio Co., Ltd. These lentiviral particles were constructed in the pLKO.1-puro vector system, which drives shRNA expression under the human U6 promoter and contains a puromycin resistance gene for selection of transduced cells. A549 and PC9 cells were infected with lentiviral particles encoding either sh-YTHDF1 or sh-PGAM1, or corresponding control shRNA, in the presence of polybrene (8 $\mu$g/ml) to enhance infection efficiency. At 48 h post-infection, cells were selected with puromycin (2 $\mu$g/ml) for 7-10 days to establish stable cell lines. The knockdown efficiency was validated by western blot analysis 72 h post-infection and prior to use in downstream assays.

Detailed information on the plasmid constructs, siRNA sequences and shRNA sequences is provided in Tables II and III. Validation of transfection efficiency for YTHDF1 and PGAM1 modulations in A549 and PC9 cells is shown in Fig. S1.

*Reverse transcription-quantitative PCR (RT-qPCR).* Total RNA was extracted from cells using the SteadyPure Mag Tissue & Cell RNA Extraction Kit (cat. no. AG21207; Hunan Accurate Bio-Medical Technology Co., Ltd.). cDNA was synthesized using the Evo M-MLV Reverse Transcription Premix Kit (cat. no. AG11728; Hunan Accurate Bio-Medical Technology Co., Ltd.) according to the manufacturer's instructions. qPCR was performed using the ChamQ Universal SYBR qPCR Master Mix (cat. no. Q711; Vazyme Biotech Co., Ltd.), a ROX reference dye-containing SYBR Green I-based fluorescent dye system. The reactions were performed using an Applied Biosystems™ PCR thermocycler (Thermo Fisher Scientific, Inc.) with three technical replicates (41). The thermal cycling conditions were as follows: Initial denaturation at 95˚C for 30 sec, followed by 40 cycles of denaturation at 95˚C for 5 sec, and annealing/extension at 60˚C for 30 sec. GAPDH was used as the internal reference gene and the relative expression levels of target genes were calculated using the $2^{-\Delta\Delta Cq}$ method. The specific oligonucleotide sequences used for PCR are shown in Table IV.

*Western blotting.* Total proteins were extracted from cells using RIPA lysis buffer (cat. no. 89901; ThermoFisher Scientific, Inc.). Protein concentration was determined using the BCA Protein Assay Kit (cat. no. 23227; Thermo Fisher Scientific, Inc.) according to the manufacturer's instructions. Equal amounts of protein (30 $\mu$g per lane) were separated by 10% SDS-PAGE and subsequently transferred onto PVDF membranes (MilliporeSigma). The membranes were blocked with 5% non-fat dry milk (cat. no. P0216; Beyotime Biotechnology) in TBST containing 0.1% Tween-20 (cat. no. ST671; Beyotime Biotechnology) for 1 h at room temperature. The membranes were incubated with specific primary antibodies at 4˚C overnight. Subsequently, the membranes were incubated with HRP-conjugated goat anti-rabbit IgG (H+L) secondary antibody (1:5,000; cat. no. SA00001-2; Proteintech Group, Inc.) at

Table II. Overexpression constructs generated in the present study.

| Plasmid | Backbone | Selection | 5'MCS | 3'MCS | Insert (codon-optimized) | Insert length, bp | Plasmid length, bp |
|---|---|---|---|---|---|---|---|
| pcDNA3.1(+)-PGAM1-HA | pcDNA3.1(+) | Ampicillin | *Nhe*I | *Bam*HI | *Homo sapiens* PGAM1 (NM_002629.3) | 810 | 6,213 |
| pcDNA3.1(+)-METTL5-FLAG | pcDNA3.1(+) | Ampicillin | *Nhe*I | *Bam*HI | *Homo sapiens* METTL5 (NM_001318165.2) | 672 | 6,075 |

PGAM1, phosphoglycerate mutase 1; HA, hemagglutinin; METTL5, methyltransferase 5; MCS, multiple cloning site.

Table III. Sequences of the siRNAs and shRNAs used in cell transfection.

| Name | Sequence (5'-3') |
|---|---|
| si-PGAM1 | |
| Sense | CCACAUCUGUAGACAUCUU |
| Antisense | AAGAUGUCUACAGAUGUGG |
| si-METTL5 | |
| Sense | GCAUGUAUGCUCUAUACAA |
| Antisense | UUGUAUAGAGCAUACAUGC |
| si-YTHDF1 | |
| Sense | CCGCGUCUAGUUGUUCAUGAA |
| Antisense | UUCAUGAACAACUAGACGCGG |
| sh-YTHDF1 | GTTCGTTACATCAGAAGGATATCAAGAGTATCCTTCTGATGTAACGAACTTTTTT |
| sh-PGAM1 | CCCTTCTGGAATGAAGAAATATCAAGAGTATTTCTTCATTCCAGAAGGGTTTTTT |

PGAM1, phosphoglycerate mutase 1; METTL5, methyltransferase 5; sh/shRNA, short hairpin RNA; si/siRNA, small interfering RNA; YTHDF1, YTH $N^6$-methyladenosine RNA binding protein 1.

Table IV. Primer sequences used in reverse transcription-quantitative PCR.

| Name | Primer | Sequence (5'-3') |
|---|---|---|
| METTL5 | Forward | TGTTAGGAGCAGGGTTGTGTG |
| | Reverse | AAGCACACATCACATTGAACCAT |
| PGAM1 | Forward | ATGATGTCCCACCACCTCCGAT |
| | Reverse | ATCCTTCAGACTCTCACAGGAG |
| GAPDH | Forward | ATGAGAAGTATGACAACAGCCTCA |
| | Reverse | GAGTCCTTCCACGATACCAAAG |

METTL5, methyltransferase 5; PGAM1, phosphoglycerate mutase 1.

room temperature for 1 h. Protein bands were visualized using sensitive ECL detection kit (cat. no. PK10002; Proteintech Group, Inc.) and the band intensity was semi-quantified using ImageJ software (version 1.54; National Institutes of Health). The experiment was performed using three independent biological replicates (n=3), with β-actin serving as the loading control. The following primary antibodies were used for western blotting: Anti-METTL5 (1:1,000; cat. no. CL488-16791; Proteintech Group, Inc.), anti-PGAM1 (1:1,000; cat. no. 16126-1-AP; Proteintech Group, Inc.), anti-YTHDF1 (1:1,000; cat. no. 17479-1-AP; Proteintech Group, Inc.), anti-GLUT1 (1:1,000; cat. no. 21829-1-AP; Proteintech Group, Inc.) and anti-β-actin (1:1,000; cat. no. 60008-1-Ig; Proteintech Group, Inc.).

*Colony formation assay*. Cells were seeded in 6-well plates at a density of 200 cells/well and maintained under standard conditions (37˚C; 5% $CO_2$; humidified atmosphere). After 14 days culture, during which no additional treatments were applied, cell colonies were fixed with 95% ethanol at room temperature for 15 min and stained with 0.1% crystal violet at room temperature for 20 min. The colonies were visualized using low-magnification microscopy (CKX53; Olympus Corporation) and quantified using ImageJ software (version 1.54; National Institutes of Health). Briefly, digital images were captured and analyzed using the 'Cell Counter' (https://imagej.nih.gov/ij/plugins/cell-counter.html) plugin to mark and count clusters containing ≥50 cells, which were defined as viable colonies. Quantification was performed in a blinded manner by two independent observers. Three independent replicates (n=3) were prepared for each sample to ensure reproducibility.

*Transwell migration assay*. For the migration assay, a total of $5x10^4$ cells were cultured in serum-free DMEM/F12 (1:1) liquid medium(cat. no. BL1917A; Biosharp Life Sciences) in the upper Transwell chamber, whereas 600 $\mu$l of DMEM/F12 (1:1) medium supplemented with 10% FBS was added to the lower chamber. After 12-24 h of incubation at 37˚C in a humidified atmosphere containing 5% $CO_2$, the migrated cells were fixed with methanol at room temperature for 15 min, stained with 0.1% crystal violet for 20 min at room temperature and observed under a phase-contrast light microscope (CKX53; Olympus Corporation) at a magnification of x400. The cells were manually counted in in five randomly selected visual fields per membrane. All experimental groups

and biological replicates were seeded with an identical initial density of $5x10^4$ cells per well. Three independent replicates were prepared for each sample to ensure reproducibility.

*Analysis of the extracellular acidification rate (ECAR) and oxygen consumption rate (OCR).* The cellular metabolic parameters ECAR and OCR were measured on a Seahorse XFe96 metabolic analyzer (Agilent Technologies, Inc.). The glycolytic rate and mitochondrial function were assessed using the Agilent Seahorse XF Glycolytic Rate Assay Kit (cat. no. 103344-100) and the Seahorse XF Cell Mito Stress Test Kit (cat. no. 103015-100), respectively. The assay solution was prepared according to the manufacturer's instructions. Briefly, glucose, pyruvate, glutamine, oligomycin, rotenone/antimycin A and carbonyl cyanide 4-(trifluoromethoxy) phenylhydrazone (FCCP) were used at final concentrations of 10 mmol/l, 1 mmol/l, 2 mmol/l, 1.5 $\mu$mol/l, 0.5 $\mu$mol/l and 1 $\mu$mol/l, respectively. Injections were automatically performed by the instrument at the following timepoints: For the OCR assay, oligomycin was injected at 14 min, FCCP was injected at 35 min and Rotenone/Antimycin A was injected at 55 min. For the ECAR assay, glucose was injected at 14 min, oligomycin was injected at 35 min and 2-DG was injected at 55 min. Measurements were recorded after achieving thermal equilibrium and stable pH conditions.

*RNA stability assay.* RNA stability was assessed by exposing cells to 5 $\mu$g/ml actinomycin D at 37˚C in a humidified incubator with 5% $CO_2$ and extracting total RNA at specified intervals (0, 4 and 8 h). Temporal mRNA expression was quantified using RT-qPCR.

*Treatment with methylation inhibitor 3-deazaadenosine (DAA).* For functional validation, METTL5-overexpressing cell lines were established and treated with the methylation inhibitor 3-deazaadenosine (DAA; cat. no. HY-W013332; MedChemExpress). Cells were seeded at a density of $1x10^5$ cells per well in 6-well plates and allowed to adhere overnight under standard culture conditions (37˚C; 5% $CO_2$). The following day, cells were treated with 50 $\mu$M DAA, a concentration previously established to effectively inhibit methyltransferase activity without inducing significant cytotoxicity (42). DAA was dissolved in dimethyl sulfoxide (DMSO; final concentration ≤0.1%; cat. no. HY-Y0320C; MedChemExpress) and added directly to the culture medium. Control cells were treated with an equivalent volume of DMSO vehicle. Cells were incubated at 37˚C in a humidified atmosphere with 5% $CO_2$ for 48 h prior to harvest for downstream assays.

*Bioinformatics analysis.* Data (TCGA-LUSC, TCGA-LUAD) used for bioinformatics analysis were obtained from The Cancer Genome Atlas (TCGA) repository (https://portal.gdc.cancer.gov/). The mRNA expression patterns and prognostic importance of METTL5 and PGAM1 in NSCLC were examined using R software (https://www.r-project.org/; version 4.3.2). Differentially expressed genes (DEGs) were identified using the 'limma' package with a significance threshold of adjusted P-value <0.05 and $\log_2$ fold change ($\log_2$FC) >1. Gene expression correlation analysis was performed using the Gene Expression Profiling Interactive Analysis (GEPIA) platform (43). Potential targets of METTL5 were identified using the M6A2Target database (44).

*Statistical analysis.* All statistical analyses were performed using GraphPad Prism (version 9.5; Dotmatics) and R (https://www.r-project.org/; version 4.3). Data are presented as the mean ± standard deviation (SD). Comparisons between two groups were performed using unpaired Student's t-tests (for independent samples) or paired t-tests (for matched samples, as indicated in figure legends), whereas multi-group comparisons were performed using one-way ANOVA followed by the Bonferroni post hoc test. Survival probabilities were calculated using Kaplan-Meier analysis and differences in survival curves were assessed using the log-rank test. Gene expression correlations were quantified using Spearman's rank coefficients. All experiments were performed in triplicate. $P<0.05$ was considered to indicate a statistically significant difference.

## Results

*METTL5 is highly expressed in NSCLC and contributes to tumor progression.* Analysis of transcriptomic data obtained from TCGA revealed significantly elevated METTL5 mRNA expression levels in NSCLC (Fig. 1A). Furthermore, METTL5 mRNA expression was significantly upregulated in colon adenocarcinoma, stomach and esophageal carcinoma, pan-kidney cohort, stomach adenocarcinoma, uterine corpus endometrial carcinoma, head and neck squamous cell carcinoma, kidney renal clear cell carcinoma, LIHC, kidney chromophobe and cholangiocarcinoma (Fig. 1B). RT-qPCR and western blotting revealed consistent upregulation patterns, with lung cancer cell lines (A549, PC9 and H520) exhibiting significantly higher METTL5 mRNA and protein expression levels compared with normal pulmonary epithelial cells (Fig. 1D). Prognostic evaluation through Kaplan-Meier analysis indicated that elevated METTL5 expression was associated with reduced survival rates in patients with NSCLC (Fig. 1C).

To investigate the role of METTL5 in NSCLC pathogenesis, cell proliferation and migration were evaluated after METTL5 knockdown or overexpression. Western blotting demonstrated the successful knockdown or overexpression of METTL5 in experimental models constructed through transfection (Fig. 1E and F). The colony formation assay showed that silencing of METTL5 significantly suppressed the proliferation of A549 and PC9 lung cancer cells, whereas ectopic overexpression significantly enhanced cell proliferation (Fig. 2A and B). The Transwell migration assay showed that silencing of METTL5 significantly inhibited the migration of lung cancer cells, whereas its overexpression significantly stimulated cell migration (Fig. 2C and D). These findings collectively indicated that METTL5 serves an oncogenic role in NSCLC, positioning it as a promising diagnostic biomarker and therapeutic target.

*Identification of PGAM1 as a direct target of METTL5.* To investigate the molecular mechanisms via which METTL5 contributes to NSCLC progression, the M6A2Target database was used to predict the targets of METTL5. PGAM1 mRNA was identified as a key potential target (45). Subsequent

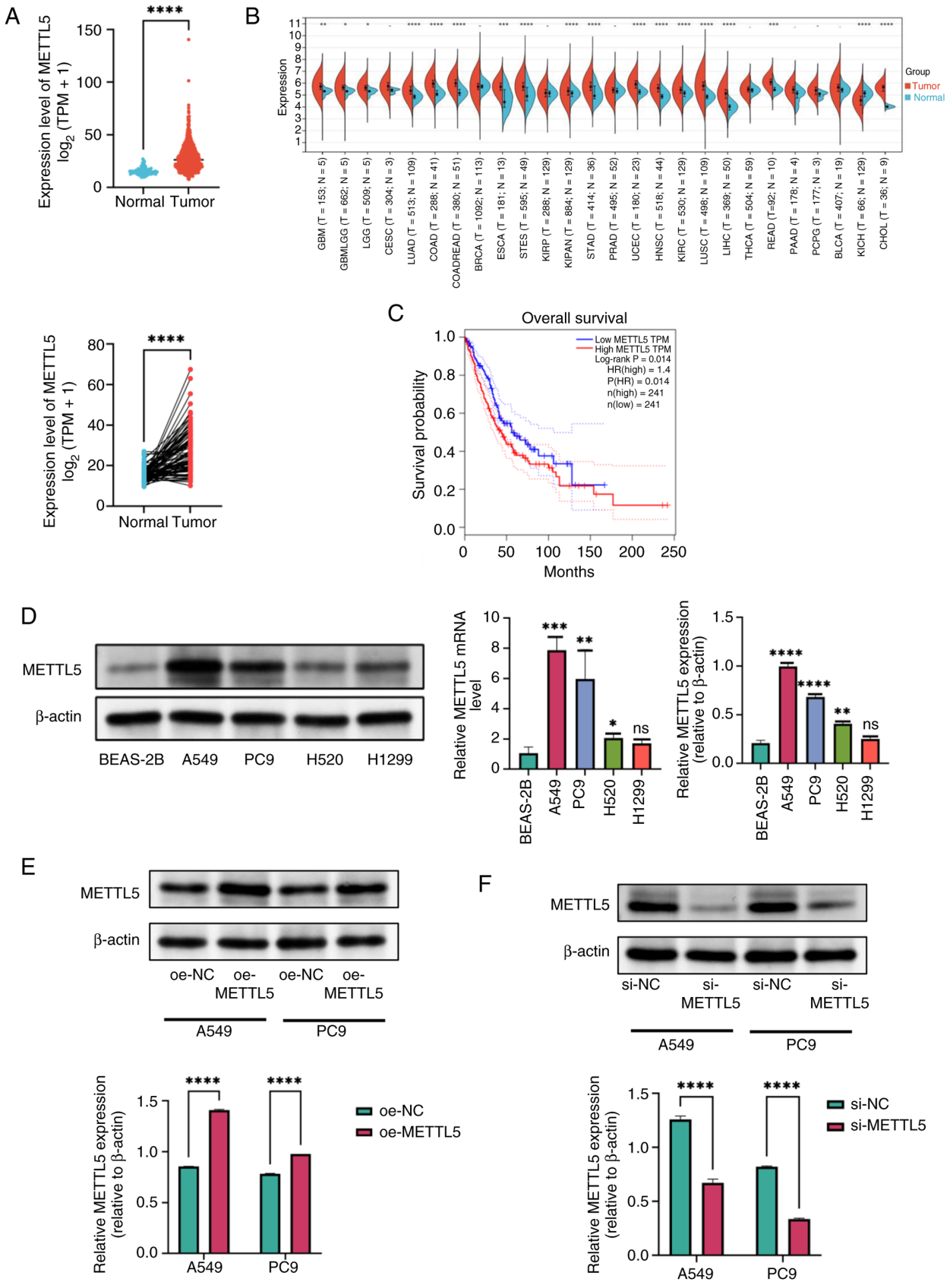


Figure 1. METTL5 is upregulated in NSCLC tissues. (A) Expression levels of METTL5 in NSCLC tissues and healthy tissues (unpaired samples) and in paired samples. (B) METTL5 expression in pan-cancer. (C) Kaplan-Meier overall survival analysis showing the survival probability of patients with NSCLC and high or low METTL5 expression (HR=1.4; log-rank P=0.014). (D) mRNA levels of METTL5 measured by reverse transcription-quantitative PCR and protein levels detected by western blot analysis in NSCLC cell lines (A549, PC9, H520 and NCI-H1299) compared with normal human lung epithelial cell line (BEAS-2B). β-actin was used as a loading control. Western blot analysis demonstrating the efficient (E) overexpression or (F) knockdown of METTL5 in A549 and PC9 cells transfected with si-METTL5 or si-NC. $^{*}$P<0.05, $^{**}$P<0.01, $^{***}$P<0.001 and $^{****}$P<0.0001. Data are presented as the mean ± SD. METTL5, methyltransferase 5; NSCLC, non-small cell lung cancer; HR, hazard ratio; TPM, transcripts per million; NC, negative control; oe, overexpression; ns, not significant; si, small interfering RNA.

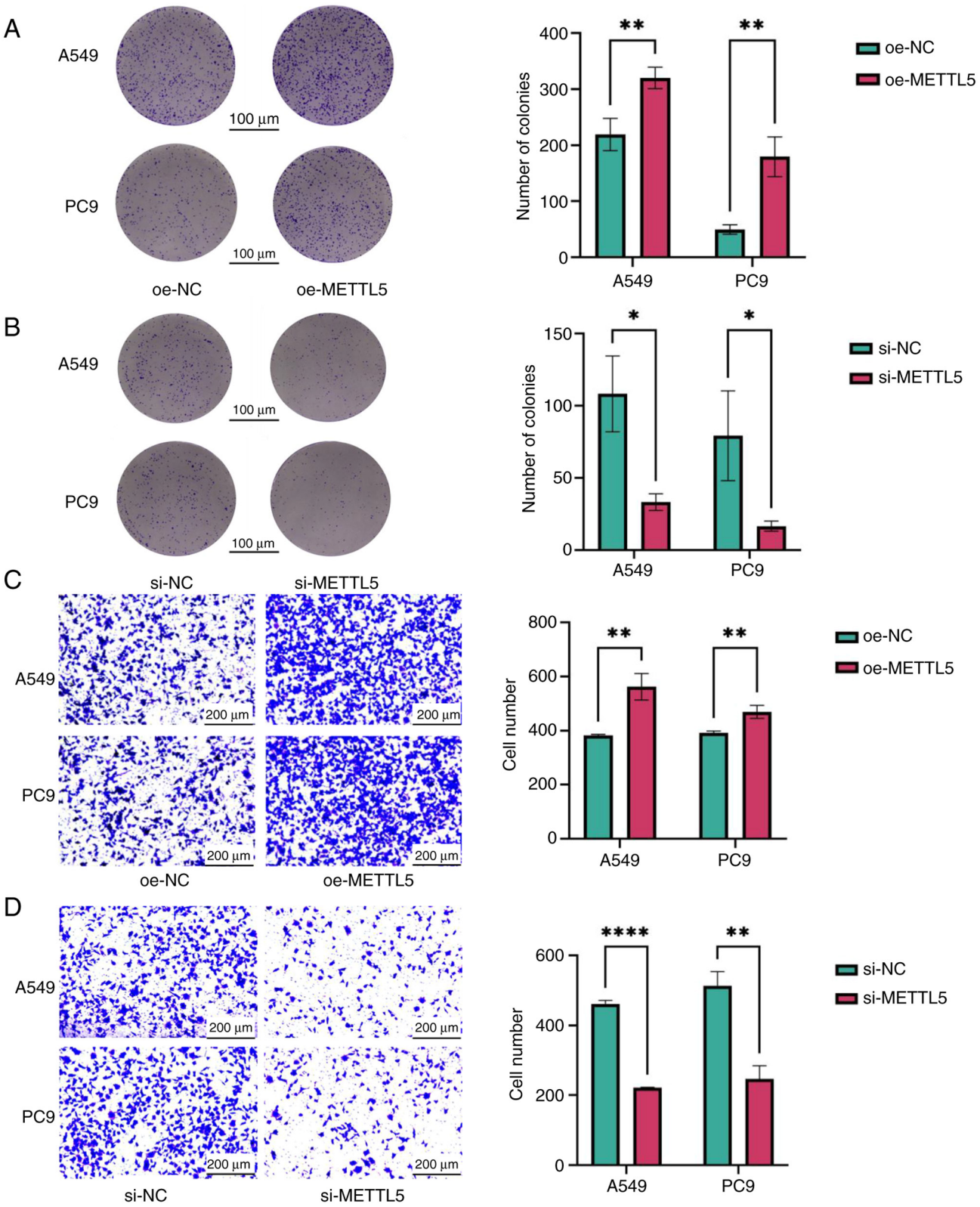


Figure 2. Colony formation and Transwell assays. Colony formation assays were performed to detect the proliferation of (A) A549 and PC9 cells with METTL5 overexpression or (B) A549 and PC9 cells with METTL5 knockdown. Colonies were stained and quantified. Transwell assays were performed to detect the migration of A549 and PC9 cells with METTL5 (C) overexpression or (D) knockdown. Representative images and quantifications are shown. $^{*}$P<0.05, $^{**}$P<0.01 and $^{****}$P<0.0001. METTL5, methyltransferase 5; oe, overexpression; Ctrl, control; si, small interfering RNA.

analysis using the GEPIA database showed a significant positive correlation between the mRNA expression levels of METTL5 and PGAM1 (R=0.45; P=5.4x10$^{-56}$; Fig. 3A). Analysis of transcriptomic data obtained from TCGA showed that the mRNA expression levels of PGAM1 were higher in NSCLC tissues compared with corresponding healthy tissues (Fig. 3B). For functional validation, METTL5-overexpressing cell lines were established and treated with the methylation inhibitor

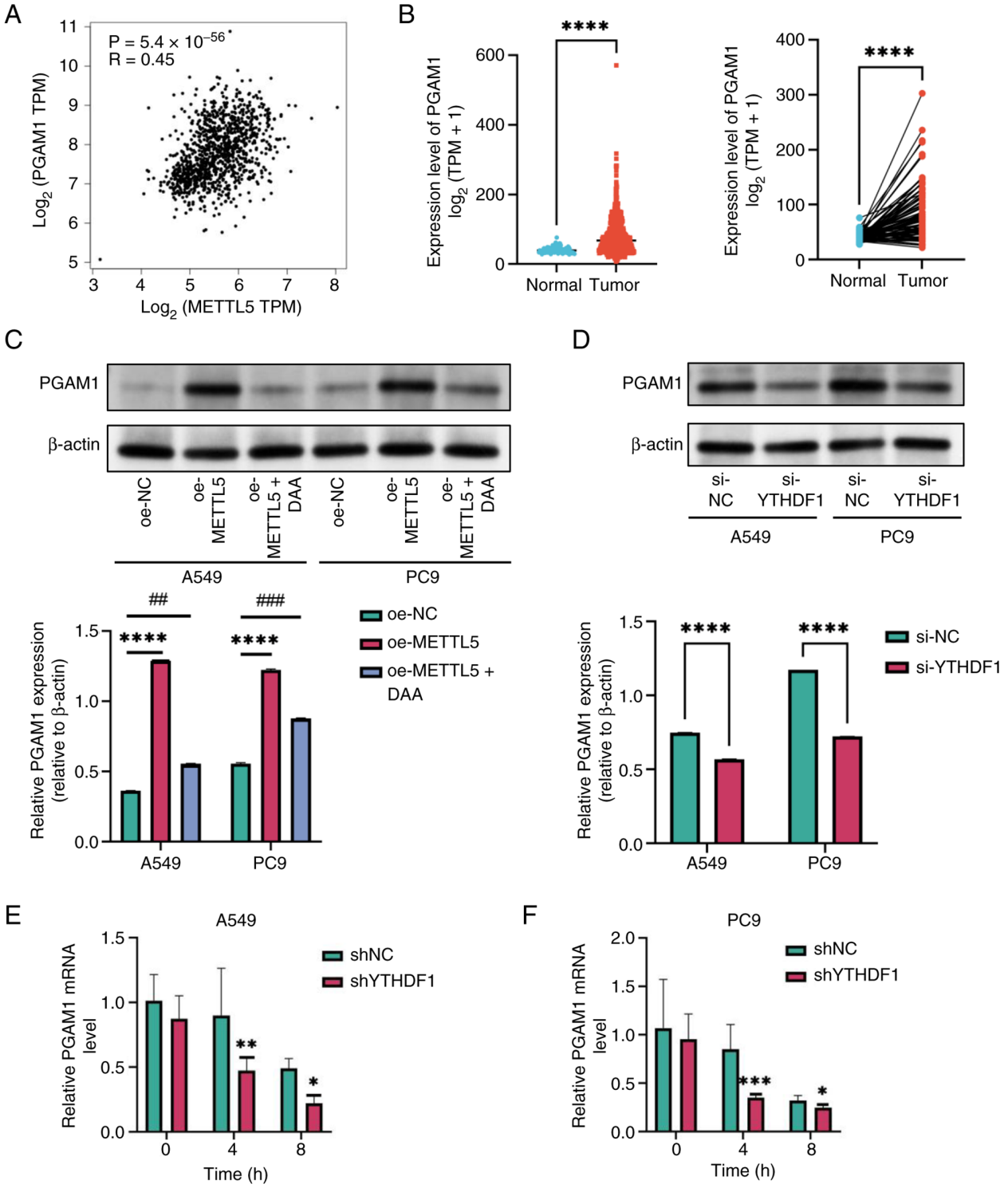


Figure 3. METTL5 regulates PGAM1 through N$^6$-methyladenosine methylation of PGAM1 mRNA. (A) Correlation analysis between METTL5 and PGAM1 expression in NSCLC tissues from The Cancer Genome Atlas database. (B) Expression levels of PGAM1 in NSCLC tissues and normal tissues and in paired samples. (C) Western blot analysis of PGAM1 protein levels in A549 and PC9 cells under different experimental conditions compared with oe-NC group. (D) PGAM1 protein expression in A549 and PC9 cells with YTHDF1 knockdown. The stability of PGAM1 mRNA was detected in YTHDF1-konckdown compared with the shNC group through reverse transcription-quantitative PCR at the indicated time after actinomycin D (5 $\mu$g/ml) treatment in (E) A549 and (F) PC9 cells. $^{*}$P<0.05, $^{**}$P<0.01, $^{***}$P<0.001, $^{****}$P<0.0001, $^{\#\#}$P<0.01 and $^{\#\#\#}$P<0.001. METTL5, methyltransferase 5; PGAM1, phosphoglycerate mutase 1; TPM, transcripts per million; NSCLC, non-small cell lung cancer; YTHDF1, YTH N$^6$-methyladenosine RNA binding protein 1; oe, overexpression; NC, negative control; DAA, 3-deazaadenosine; si, small interfering RNA; sh, short hairpin RNA.

3-deazaadenosine (DAA). Western blot analysis revealed that overexpression of METTL5 significantly increased PGAM1 protein levels compared with the negative control, while treatment with the methylation inhibitor DAA reversed this effect (Fig. 3C), indicating that PGAM1 expression is dependent on METTL5-mediated methylation. These findings collectively suggested that PGAM1 mRNA was methylated by METTL5 under physiological conditions.

*Identification of YTHDF1 as an m$^6$A reader of PGAM1.* Studies have shown that m$^6$A readers serve an important role in methylation (46,47). Based on the predictions of the M6A2Target database and Shi *et al* (48) (GSE ID: GSE136433), YTHDF1 was identified as an m$^6$A reader that recognizes and binds to methylated PGAM1 mRNA. Western blotting further confirmed these findings, indicating that PGAM1 protein expression was significantly lower in YTHDF1-silenced cells compared with control cells (Fig. 3D). These findings align with those of RNA immunoprecipitation (RIP) sequencing in previous studies (48,49), determining direct molecular interactions between YTHDF1 and PGAM1 mRNA. Furthermore, RNA stability analysis revealed that the silencing of YTHDF1 accelerated PGAM1 mRNA decay rates in NSCLC cells, indicating enhanced mRNA degradation (Fig. 3E and F) These findings collectively indicated that YTHDF1 directly recognized m$^6$A-modified PGAM1 mRNA to regulate its stability and expression.

*METTL5 and PGAM1 promote glycolysis by regulating GLUT1 expression.* As an important enzyme in glycolysis, PGAM1 mediates the interconversion between 3-phosphoglycerate (3-PGA) and 2-phosphoglycerate (2-PGA), thereby enhancing cellular energy metabolism. Through its regulatory role in maintaining equilibrium between these metabolites, PGAM1 affects ancillary metabolic processes. This enzymatic activity influences a number of biosynthetic processes, not only channeling carbon flux towards biosynthetic pathways for macromolecule production but also maintaining cellular redox homeostasis. Furthermore, emerging evidence indicates that PGAM1 regulates mitochondrial function and shapes the tumor immune microenvironment, collectively driving malignant proliferation and metastatic spread in neoplastic tissues (50-52). In the present study, the functional importance of the METTL5/PGAM1 axis in NSCLC pathogenesis and energy metabolism was examined. Metabolic flux analysis showed that PGAM1-knockdown cells exhibited a decreased ECAR but an increased OCR (Fig. 4F and G).

Studies have shown that overexpression of GLUT1 and GLUT3 can promote glucose uptake in tumor cells and lead to chemoresistance by activating oncogenic signaling pathways, such as the PI3K/AKT pathway (53,54). Hexokinase 2 (HK2) is a key enzyme in glycolysis initiation, and its activation can drive tumor metabolism toward glycolysis (55,56). Phosphofructokinase, platelet (PFKP) and 6-phosphofructo-2-kinase/fructose-2,6-bisphosphatases (PFKFB)-3 serve important roles in tumor glycolysis, inducing high glycolytic activity, which may lead to drug resistance (57). To determine the molecular mechanism of METTL5/PGAM1-mediated glycolysis, correlation analysis was performed between PGAM1 expression and GLUT1, GLUT3, HK2, PFKP or PFKFB3 expression (Fig. 4A-E). The correlation between PGAM1 and GLUT1 expression exhibited the highest significance ($P=4.12x10^{-183}$; R=0.6). This finding was validated by detecting protein expression. Knockdown of PGAM1 significantly decreased GLUT1 protein expression in NSCLC cells, whereas its overexpression had the opposite effect (Fig. 5A).

Furthermore, the effects of METTL5 on GLUT1 expression were investigated. Overexpression of METTL5 significantly upregulated GLUT1 expression in NSCLC cells, whereas its knockdown significantly downregulated GLUT1 expression (Fig. 5B). In rescue experiments, compared with the METTL5-knockdown group, GLUT1 protein expression was elevated in cells with METTL5 knockdown combined with PGAM1 overexpression, implying that PGAM1 overexpression partially reversed the downregulation of GLUT1 caused by METTL5 deficiency. This supported the present hypothesis that PGAM1 acts downstream of METTL5 in regulating GLUT1 expression (Fig. 5C).

## Discussion

As a hallmark of malignant transformation, the Warburg effect refers to tumor cells predominantly using glycolysis rather than oxidative phosphorylation for energy production, even under normoxic conditions (58). Although the underlying mechanisms are multifaceted, studies have indicated that this metabolic reprogramming supports the proliferation, metastatic spread and invasive potential of tumor cells (59-61). As a predominant RNA modification, m$^6$A serves an important role in regulating both coding and non-coding RNAs. A previous study has highlighted its notable role in carcinogenesis, particularly through the modulation of metabolic pathways in a number of malignancies (62). For example, in colorectal carcinoma, the methyltransferase VIRMA enhances m$^6$A-mediated methylation of HK2 mRNA, leading to elevated HK2 mRNA expression and increased transcript stability. This process ultimately promotes aerobic glycolysis in cancer cells and augments their malignant potential (63). Furthermore, in gastric cancer, the stability and expression levels of heparin binding growth factor (HDGF) mRNA are enhanced through m$^6$A modification mediated by METTL3, followed by its interaction with insulin-like growth factor 2 mRNA-binding protein 3. Nuclear HDGF binds to the promoter regions of GLUT4 and enolase 2, leading to elevated levels of glycolytic enzymes, thereby stimulating glycolysis, tumor growth and hepatic metastasis in gastric cancer (64). Yang *et al* (65) demonstrated that elevated hepatitis B virus X-interacting protein (HBXIP) expression enhanced glycolytic activity in HCC cells, thereby increasing their malignant potential. This effect was mediated through HBXIP-induced upregulation of METTL3. In METTL3-overexpressing hepatocellular carcinoma (HCC) cells, elevated m$^6$A methylation of hypoxia inducible factor 1-α was observed, and this led to the activation of downstream glycolytic enzymes and a corresponding increase in the invasiveness of HCC cells (65).

METTL5 is an 18S ribosomal RNA (rRNA)-specific m$^6$A methyltransferase. Its main function is to regulate ribosomal translation by catalyzing m$^6$A modification at the A1832 site in 18S rRNA (35). METTL5 has been reported to be markedly upregulated in a number of cancer types, including breast cancer and HCC (36,66,67). Furthermore, METTL5 has been shown to regulate metabolic reprogramming. In HCC, METTL5 promotes fatty acid β-oxidation and the Warburg effect by targeting acyl-coA synthetase long chain family member 4 (ACSL4). ACSL4 encodes a key metabolic enzyme that activates fatty acids by catalyzing their conversion to acyl-CoA esters, thereby supporting the energy demand of tumor cells (66). The present study demonstrated that METTL5

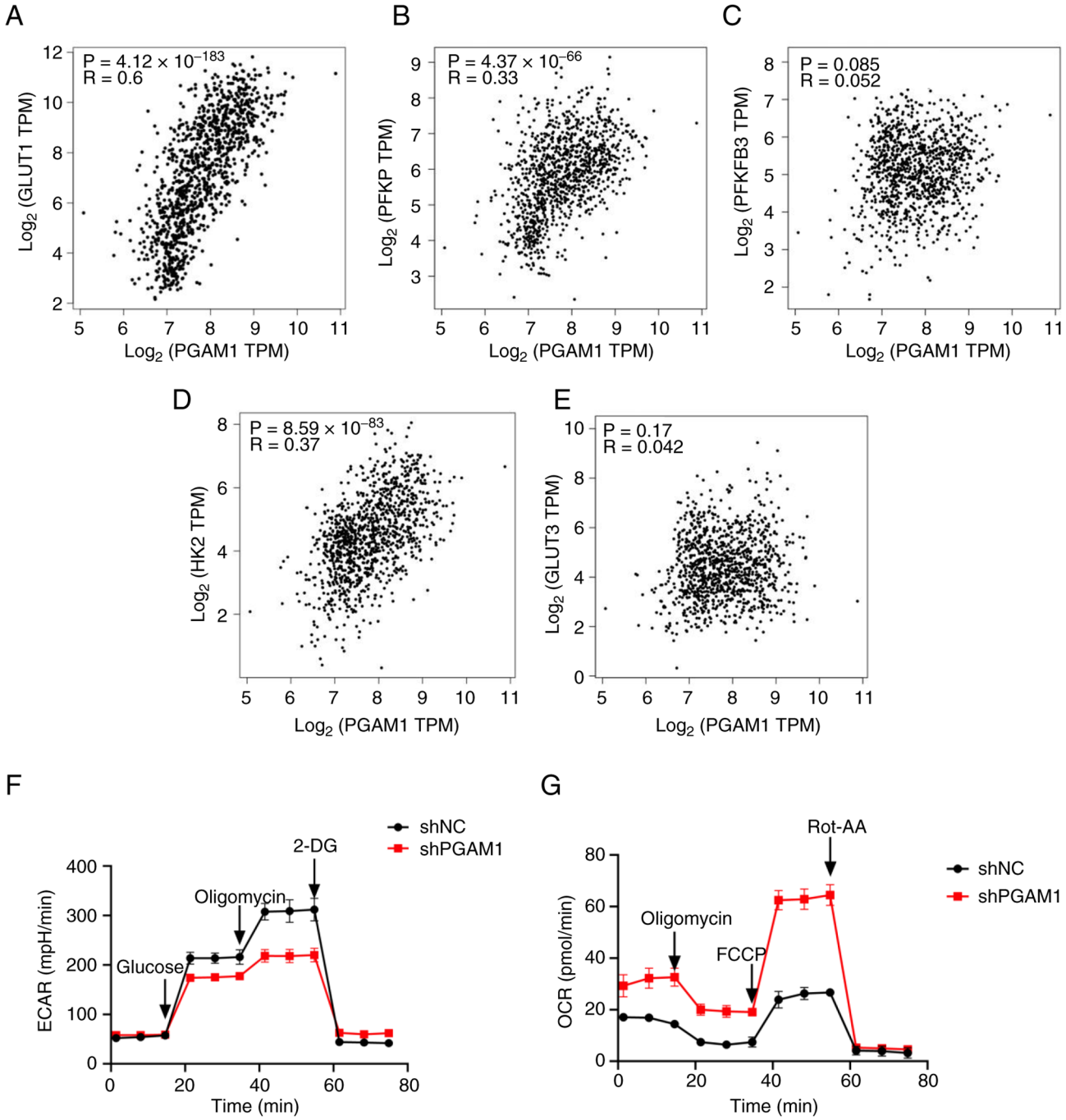


Figure 4. Correlation analysis and metabolic flux analysis. Correlation analysis between PGAM1 expression and (A) GLUT1, (B) PFKP, (C) PFKFB3, (D) HK2 and (E) GLUT3 expression in non-small cell lung cancer tissues from The Cancer Genome Atlas database. (F) ECAR and (G) OCR profiles were measured in PGAM1-knockdown A549 cells. The metabolic inhibitors were injected sequentially at different time points as indicated. TPM, transcripts per million; PGAM1, phosphoglycerate mutase 1; SLC2A1, solute carrier family 2 member 1; GLUT, glucose transporter; PFKP, phosphofructokinase, platelet; PFKFB, 6-phosphofructo-2-kinase/fructose-2,6-bisphosphatases; HK2, hexokinase 2; ECAR, extracellular acidification rate; OCR, oxygen consumption rate; sh, short hairpin RNA; Rot-AA,rotenone/antimycin A; 2-DG, 2-deoxy-D-glucose; FCCP, carbonyl cyanide 4-(trifluoromethoxy)phenylhydrazone.

enhanced glycolytic activity and tumor cell proliferation in NSCLC, thereby promoting NSCLC progression.

PGAM1 serves as a key metabolic catalyst in facilitating the interconversion between 3-PGA and 2-PGA during glycolysis. By regulating the flux of these intermediates, PGAM1 supports the generation of energy and provides essential precursors for serine synthesis, the pentose phosphate pathway and phospholipid metabolism (68). In certain tumors, PGAM1 not only exhibits enzymatic activity but also participates in enzyme-independent metabolic regulation. For example, in breast cancer, PGAM1 interacts with α-smooth muscle actin through direct binding, enhancing the migration and metastatic spread of cancer cells through non-catalytic mechanisms involving protein-protein interfaces. This interaction is independent of PGAM1 metabolic activity; the enzymatically inactive H186R mutant retains ACTA2 binding, whereas a mutant lacking amino acids 201-210 fails to interact despite maintaining full enzymatic function. By acting as a

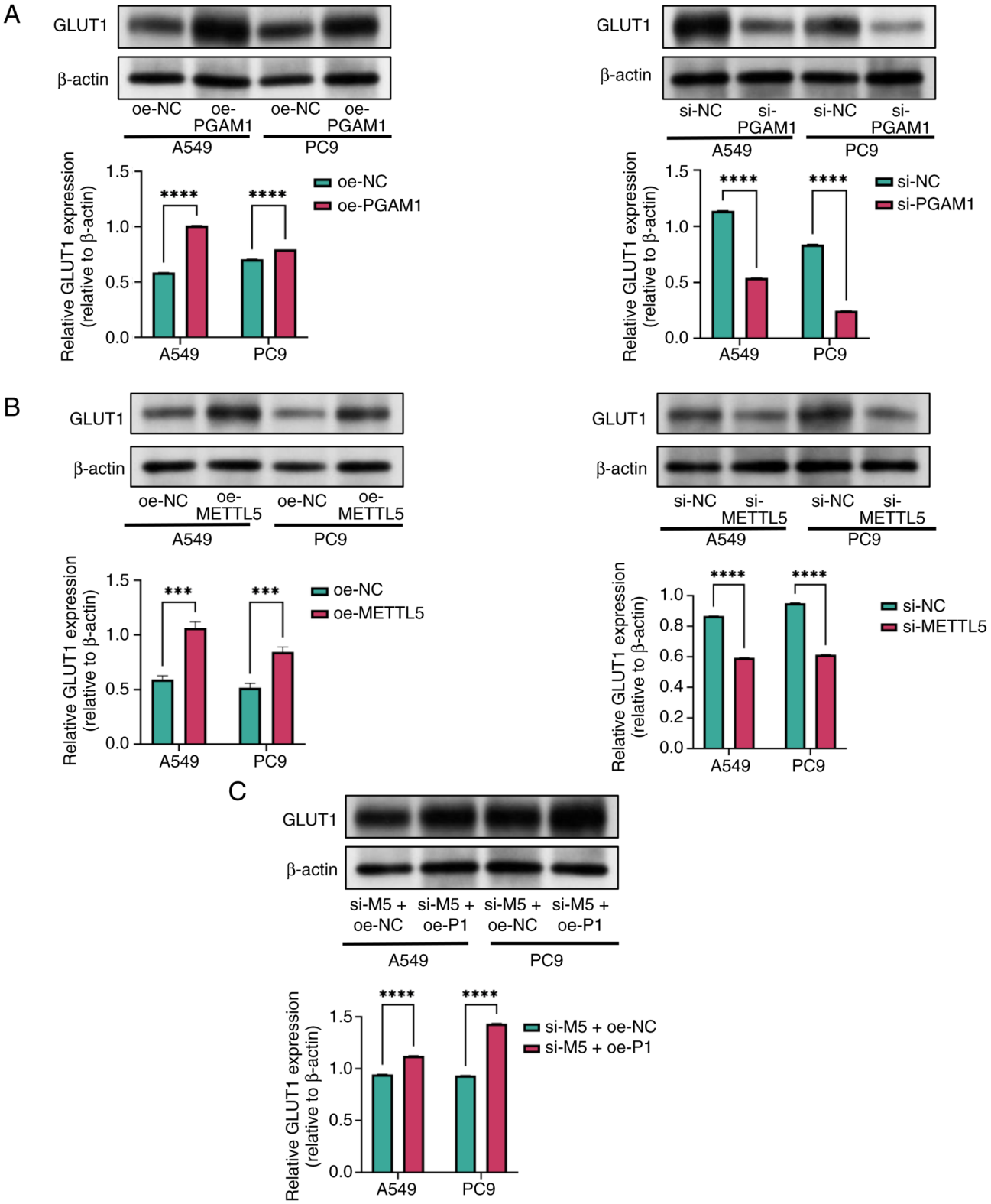


Figure 5. Western blot analysis of GLUT1 protein levels under different experimental conditions. (A) GLUT1 protein expression was significantly reduced in PGAM1-knockdown cell lines and significantly elevated in PGAM1-overexpressing cell lines. (B) GLUT1 protein expression was significantly reduced in METTL5-knockdown cell lines and significantly elevated in METTL5-overexpressing cell lines. (C) GLUT1 protein expression was upregulated in METTL5-silenced cells co-transfected with PGAM1 overexpression plasmid. β-actin was used as the loading control. ***P<0.001 and ****P<0.0001. GLUT1, glucose transporter type 1; PGAM1, phosphoglycerate mutase 1; METTL5, methyltransferase 5; NC, negative control; oe, overexpression; si, small interfering RNA.

structural adaptor, PGAM1 directly modulates actin filament assembly and cytoskeletal dynamics, thereby promoting cell motility (51). PGAM1 has emerged as a promising therapeutic target for cancer and marked advancements have been made in designing PGAM1 inhibitors. For example, HKB99 is a novel allosteric PGAM1-targeted compound with potent suppressive

effects on both tumor progression and metastatic spread in NSCLC. In addition, it has exhibited therapeutic potential in erlotinib-resistant tumors (69).

As an important glucose transporter, GLUT1 regulates cellular glucose uptake and frequently acts as a metabolic bottleneck in malignant tumors. These key functions of GLUT1 are observed in a number of malignancies. For example, GLUT1-enriched cancer-associated fibroblasts can drive metastatic niche formation through metabolic reprogramming in ovarian carcinoma (70). In LUAD, the long non-coding RNA GAS6-AS1 blocks glucose metabolic reprogramming by inhibiting GLUT1 expression, thereby inhibiting tumor progression (71). In glioblastoma, GLUT1 inhibition can reduce the excretion of lactate produced by tumor glycolysis, thereby improving the immunosuppressive tumor microenvironment (72). These findings collectively indicate that the METTL5/PGAM1 signaling axis facilitates glycolytic metabolism and tumor progression by regulating GLUT1 in NSCLC.

The present study demonstrated that METTL5 was markedly upregulated in NSCLC, with this upregulation being associated with unfavorable clinical outcomes. METTL5 promoted the proliferation, migration and glycolytic activity of NSCLC cells *in vitro*, regulating the expression of PGAM1 mRNA through $m^6A$ modification. PGAM1 mRNA could also be recognized and bound by YTHDF1 to inhibit its degradation. PGAM1 overexpression results in the upregulation of GLUT1, thereby enhancing glycolysis and lactate production in NSCLC cells. PGAM1 catalyzes the key reaction in glycolysis, converting 3-PGA to 2-PGA, increasing GLUT1 expression, accelerating glucose uptake efficiency and providing sufficient substrates for cells (68). Therefore, we hypothesized that the METTL5/PGAM1/GLUT1 axis promoted NSCLC progression by reprogramming glucose metabolism.

Despite notable findings, the present study had certain limitations. While the colony formation assays demonstrated the impact of METTL5 on clonal expansion, the integration of MTT analysis will be considered in future studies to validate these effects across different proliferation metrics. The colony formation assay was specifically selected to assess the self-renewal and sustained proliferation capacities of cells, which are important in understanding tumorigenicity. This approach aligned with the objective of the present study to explore the role of METTL5 in cancer stemness and metastatic potential. Furthermore, due to the established association between clonogenicity and tumor aggressiveness (73), the present study prioritized this endpoint to provide mechanistic insights into the contribution of METTL5 to NSCLC progression. Nevertheless, it should be recognized that MTT assays may complement the present findings by capturing shorter-term proliferation rates. Although the biological function of METTL5 in NSCLC cells was investigated using RT-qPCR, western blotting and cellular functional assays, further validation in animal or clinical tissue samples is required. While *in vitro* cell line experiments provide valuable mechanistic insights, they exhibit inherent limitations in fully recapitulating the complexity of human tumors, including tumor heterogeneity, the tumor microenvironment and systemic physiological regulation. In the future, the authors plan to validate key findings in clinical NSCLC tissue samples and establish animal models to evaluate *in vivo* tumorigenicity and therapeutic potential. In addition, small-molecule inhibitors targeting METTL5 or its downstream effectors (such as PGAM1) are being screened in preclinical models, with the aim of identifying potential strategies for metabolism-targeted therapy in NSCLC. These complementary approaches will allow the gap between *in vitro* observations and clinical reality to be closed, thereby enhancing the translational importance of the present study.

Overall, the mechanistic interactions between METTL5 and PGAM1, particularly those contributing to $m^6A$ modification, warrant further investigation. The $m^6A$ levels of PGAM1 transcripts were not directly quantified in the present study. Instead, inferences were drawn from protein expression patterns after DAA treatment. In future studies, methylated RIP sequencing may be used to directly quantify the $m^6A$ levels of PGAM1 mRNA. To assess whether YTHDF1 is an $m^6A$ reader of PGAM1, bioinformatics analysis and western blotting were used to indirectly determine the association between YTHDF1 and PGAM1. Although previous studies (48,49) have reported the use of RIP sequencing, RNA pulldown experiments may be used to elucidate the association between YTHDF1 and PGAM1. In addition, the METTL5/PGAM1 axis may target proteins other than GLUT1 to promote glycolysis. Notably, while HK2 and PFKP showed more modest but statistically significant correlations with PGAM1 expression (R=0.37 and R=0.33, respectively) compared with GLUT1 (R=0.6), these findings suggested that HK2 and PFKP may also be functionally associated with the METTL5/PGAM1 axis, potentially through indirect mechanisms such as metabolic reprogramming or transcriptional network modulation. These potential targets, especially HK2 and PFKP, should be identified to further understand the role of the METTL5/PGAM1 axis in NSCLC progression.

**Acknowledgements**

Not applicable.

**Funding**

The present study was funded by the Changzhou High-Level Medical Talents Training Project (grant no. 2022CZBJ069), the Changzhou Sci & Tech Program (grant no. CZ20220025), the '333 Project' of Jiangsu Province (grant no. BRA2020157), the 333 High-Level Talent Training Project (grant no. 2022-2) and the Science and Technology Development Fund of Nanjing Medical University (grant no. NMUB20250013).

**Availability of data and materials**

The data generated in the present study may be requested from the corresponding author.

**Authors' contributions**

YS, ZG and XD conceived and designed the experiments. Data collection and analysis was performed by KY, ML and QW. ZG and ML also analyzed and interpreted the data and prepared all figures for publication. KY and QW provided financial and

technical support. The first draft of the manuscript was written by ML and ZG and revised by YS. All authors commented on previous versions of the manuscript. All authors have read and approved the final version of the manuscript. YS and ZG confirm the authenticity of all the raw data.

**Ethics approval and consent to participate**

Not applicable.

**Patient consent for publication**

Not applicable.

**Competing interests**

The authors declare that they have no competing interests.

**References**


1. Sung H, Ferlay J, Siegel RL, Laversanne M, Soerjomataram I, Jemal A and Bray F: Global cancer statistics 2020: GLOBOCAN estimates of incidence and mortality worldwide for 36 cancers in 185 countries. CA Cancer J Clin 71: 209-249, 2021.
2. Molina JR, Yang P, Cassivi SD, Schild SE and Adjei AA: Non-small cell lung cancer: Epidemiology, risk factors, treatment, and survivorship. Mayo Clin Proc 83: 584-594, 2008.
3. Lobb RJ, Visan KS, Wu LY, Norris EL, Hastie ML, Everitt S, Yang IA, Bowman RV, Siva S, Larsen JE, *et al*: An epithelial-to-mesenchymal transition induced extracellular vesicle prognostic signature in non-small cell lung cancer. Commun Biol 6: 68, 2023.
4. Richards TB, Henley SJ, Puckett MC, Weir HK, Huang B, Tucker TC and Allemani C: Lung cancer survival in the United States by race and stage (2001-2009): Findings from the CONCORD-2 study. Cancer 123 (Suppl 24): S5079-S5099, 2017.
5. Wang Q, Li J, Zhu J, Mao J, Duan C, Liang X, Zhu L, Zhu M, Zhang Z, Lin F and Guo R: Genome-wide CRISPR/Cas9 screening for therapeutic targets in NSCLC carrying wild-type TP53 and receptor tyrosine kinase genes. Clin Transl Med 12: e882, 2022.
6. Zhang J, Song Z, Zhang Y, Zhang C, Xue Q, Zhang G and Tan F Recent advances in biomarkers for predicting the efficacy of immunotherapy in non-small cell lung cancer. Front Immunol 16: 1554871, 2025.
7. Sun L, Suo C, Li ST, Zhang H and Gao P: Metabolic reprogramming for cancer cells and their microenvironment: Beyond the Warburg Effect. Biochim Biophys Acta Rev Cancer 1870: 51-66, 2018.
8. Yoshida GJ: Metabolic reprogramming: The emerging concept and associated therapeutic strategies. J Exp Clin Cancer Res 34: 111, 2015.
9. Lebelo MT, Joubert AM and Visagie MH: Warburg effect and its role in tumourigenesis. Arch Pharm Res 42: 833-847, 2019.
10. Liberti MV and Locasale JW: The Warburg effect: How does it benefit cancer cells? Trends Biochem Sci 41: 211-218, 2016.
11. Gao X, Zhou S, Qin Z, Li D, Zhu Y and Ma D: Upregulation of HMGB1 in tumor-associated macrophages induced by tumor cell-derived lactate further promotes colorectal cancer progression. J Transl Med 21: 53, 2023.
12. Jin X, Zhang N, Yan T, Wei J, Hao L, Sun C, Zhao H and Jiang S: Lactate-mediated metabolic reprogramming of tumor-associated macrophages: Implications for tumor progression and therapeutic potential. Front Immunol 16: 1573039, 2025.
13. Qian J, Gong ZC, Zhang YN, Wu HH, Zhao J, Wang LT, Ye LJ, Liu D, Wang W, Kang X, *et al*: Lactic acid promotes metastatic niche formation in bone metastasis of colorectal cancer. Cell Commun Signal 19: 9, 2021.
14. Gu XY, Yang JL, Lai R, Zhou ZJ, Tang D, Hu L and Zhao LJ: Impact of lactate on immune cell function in the tumor microenvironment: Mechanisms and therapeutic perspectives. Front Immunol 16: 1563303, 2025.
15. Watson MJ, Vignali PDA, Mullett SJ, Overacre-Delgoffe AE, Peralta RM, Grebinoski S, Menk AV, Rittenhouse NL, DePeaux K, Whetstone RD, *et al*: Metabolic support of tumour-infiltrating regulatory T cells by lactic acid. Nature 591: 645-651, 2021.
16. Jin J, Yan P, Wang D, Bai L, Liang H, Zhu X, Zhu H, Ding C, Wei H and Wang Y: Targeting lactylation reinforces NK cell cytotoxicity within the tumor microenvironment. Nat Immunol 26L: 1099-1112, 2025.
17. Gu J, Zhou J, Chen Q, Xu X, Gao J, Li X, Shao Q, Zhou B, Zhou H, Wei S, *et al*: Tumor metabolite lactate promotes tumorigenesis by modulating MOESIN lactylation and enhancing TGF-β signaling in regulatory T cells. Cell Rep 39: 110986, 2022.
18. Xie Y, Wang M, Qiao L, Qian Y, Xu W, Sun Q, Luo S and Li C: Photothermal-Enhanced Dual Inhibition of Lactate/Kynurenine metabolism for promoting tumor immunotherapy. Small Methods 8: e2300945, 2024.
19. Chen S, Xu Y, Zhuo W and Zhang L: The emerging role of lactate in tumor microenvironment and its clinical relevance. Cancer Lett 590: 216837, 2024.
20. Alarcón CR, Lee H, Goodarzi H, Halberg N and Tavazoie SF: N6-methyladenosine marks primary microRNAs for processing. Nature 519: 482-485, 2015.
21. Zhao BS, Roundtree IA and He C: Post-transcriptional gene regulation by mRNA modifications. Nat Rev Mol Cell Biol 18: 31-42, 2017.
22. Huang Q, Mo J, Liao Z, Chen X and Zhang B: The RNA $m^6A$ writer WTAP in diseases: Structure, roles, and mechanisms. Cell Death Dis 13: 852, 2022.
23. Zhou H, Yin K, Zhang Y, Tian J and Wang S: The RNA m6A writer METTL14 in cancers: Roles, structures, and applications. Biochim Biophys Acta Rev Cancer 1876: 188609, 2021.
24. Zeng C, Huang W, Li Y and Weng H: Roles of METTL3 in cancer: Mechanisms and therapeutic targeting. J Hematol Oncol 13: 117, 2020.
25. Gao Z, Zha X, Li M, Xia X and Wang S: Insights into the $m^6A$ demethylases FTO and ALKBH5: Structural, biological function, and inhibitor development. Cell Biosci 14: 108, 2024.
26. Lan Q, Liu PY, Haase J, Bell JL, Hüttelmaier S and Liu T: The critical role of RNA $m^6A$ methylation in cancer. Cancer Res 79: 1285-1292, 2019.
27. Shi H, Wei J and He C: Where, When, and How: Context-dependent functions of RNA methylation writers, readers, and erasers. Mol Cell 74: 640-650, 2019.
28. Zaccara S, Ries RJ and Jaffrey SR: Reading, writing and erasing mRNA methylation. Nat Rev Mol Cell Biol 20: 608-624, 2019.
29. Wu X, Chen H, Li K, Zhang H, Li K and Tan H: The biological function of the N6-Methyladenosine reader YTHDC2 and its role in diseases. J Transl Med 22: 490, 2024.
30. Huang H, Weng H and Chen J: m6A Modification in coding and Non-coding RNAs: Roles and therapeutic implications in cancer. Cancer Cell 37: 270-288, 2020.
31. Yi YC, Chen XY, Zhang J and Zhu JS: Novel insights into the interplay between m6A modification and noncoding RNAs in cancer. Mol Cancer 19: 121, 2020.
32. Zhang Y, Chen Y, Guo Q, Zhang Y and Liu A: Fat mass and obesity-associated protein (FTO)-induced upregulation of flotillin-2 (FLOT2) contributes to cancer aggressiveness in diffuse large B-cell lymphoma (DLBCL) via activating the PI3K/Akt/mTOR signal pathway. Arch Biochem Biophys 758: 110072, 2024.
33. Wang Y, Hong Z, Song J, Zhong P and Lin L: METTL3 promotes drug resistance to oxaliplatin in gastric cancer cells through DNA repair pathway. Front Pharmacol 14: 1257410, 2023.
34. Deng LJ, Deng WQ, Fan SR, Chen MF, Qi M, Lyu WY, Qi Q, Tiwari AK, Chen JX, Zhang DM and Chen ZS: m6A modification: Recent advances, anticancer targeted drug discovery and beyond. Mol Cancer 21: 52, 2022.
35. van Tran N, Ernst FGM, Hawley BR, Zorbas C, Ulryck N, Hackert P, Bohnsack KE, Bohnsack MT, Jaffrey SR, Graille M and Lafontaine DLJ: The human 18S rRNA m6A methyltransferase METTL5 is stabilized by TRMT112. Nucleic Acids Res 47: 7719-7733, 2019.
36. Xia P, Zhang H, Lu H, Xu K, Jiang X, Jiang Y, Gongye X, Chen Z, Liu J, Chen X, *et al*: METTL5 stabilizes c-Myc by facilitating USP5 translation to reprogram glucose metabolism and promote hepatocellular carcinoma progression. Cancer Commun (Lond) 43: 338-364, 2023.
37. Zhang W, Chen Y, Zeng Z, Peng Y, Li L, Hu N, Gao X, Cai W, Yin L, Xu Y, *et al*: The novel m6A writer METTL5 as prognostic biomarker probably associating with the regulation of immune microenvironment in kidney cancer. Heliyon 8: e12078, 2022.
38. Li X, Yang G, Ma L, Tang B and Tao T: N6-methyladenosine (m6A) writer METTL5 represses the ferroptosis and antitumor immunity of gastric cancer. Cell Death Discov 10: 402, 2024.

39. Zhou Z, Li Y, Chen S, Xie Z, Du Y, Liu Y, Shi Y, Lin X, Zeng X, Zhao H and Chen G: GLUT1 promotes cell proliferation via binds and stabilizes phosphorylated EGFR in lung adenocarcinoma. Cell Commun Signal 22: 303, 2024.
40. Ren Z, Zhao J, Li S and Yuan H: Targeting glucose transporter 1 (GLUT1) in cancer: Molecular mechanisms and nanomedicine applications. Int J Nanomedicine 20: 11859-11879, 2025.
41. Livak KJ and Schmittgen TD: Analysis of relative gene expression data using real-time quantitative PCR and the 2(-Delta Delta C(T)) method. Methods 25: 402-408, 2001.
42. Lv YB, Chen C, Yu QM, Lyu L, Peng YF and Tan XD: Synthesis and biological evaluation of novel pentanediamide derivatives as S-adenosyl-l-homocysteine hydrolase inhibitors. Bioorg Med Chem Lett 72: 128880, 2022.
43. Tang Z, Li C, Kang B, Gao G, Li C and Zhang Z: GEPIA: A web server for cancer and normal gene expression profiling and interactive analyses. Nucleic Acids Res 45: W98-W102, 2017.
44. Deng S, Zhang H, Zhu K, Li X, Ye Y, Li R, Liu X, Lin D, Zuo Z and Zheng J: M6A2Target: A comprehensive database for targets of m6A writers, erasers and readers. Brief Bioinform 22: bbaa055, 2021.
45. Sepich-Poore C, Zheng Z, Schmitt E, Wen K, Zhang ZS, Cui XL, Dai Q, Zhu AC, Zhang L, Sanchez Castillo A, *et al*: The METTL5-TRMT112 N6-methyladenosine methyltransferase complex regulates mRNA translation via 18S rRNA methylation. J Biol Chem 298: 101590, 2022.
46. He L, Li H, Wu A, Peng Y, Shu G and Yin G: Functions of N6-methyladenosine and its role in cancer. Mol Cancer 18: 176, 2019.
47. Fang X, Li M, Yu T, Liu G and Wang J: Reversible N6-methyladenosine of RNA: The regulatory mechanisms on gene expression and implications in physiology and pathology. Genes Dis 7: 585-597, 2020.
48. Shi Y, Fan S, Wu M, Zuo Z, Li X, Jiang L, Shen Q, Xu P, Zeng L, Zhou Y, *et al*: YTHDF1 links hypoxia adaptation and non-small cell lung cancer progression. Nat Commun 10: 4892, 2019.
49. Zhang X, Su T, Wu Y, Cai Y, Wang L, Liang C, Zhou L, Wang S, Li XX, Peng S, *et al*: N6-Methyladenosine reader YTHDF1 promotes stemness and therapeutic resistance in hepatocellular carcinoma by enhancing NOTCH1 expression. Cancer Res 84: 827-840, 2024.
50. Sun Q, Li S, Wang Y, Peng H, Zhang X, Zheng Y, Li C, Li L, Chen R, Chen X, *et al*: Phosphoglyceric acid mutase-1 contributes to oncogenic mTOR-mediated tumor growth and confers non-small cell lung cancer patients with poor prognosis. Cell Death Differ 25: 1160-1173, 2018.
51. Zhang D, Jin N, Sun W, Li X, Liu B, Xie Z, Qu J, Xu J, Yang X, Su Y, *et al*: Phosphoglycerate mutase 1 promotes cancer cell migration independent of its metabolic activity. Oncogene 36: 2900-2909, 2017.
52. Luo JQ, Yang TW, Wu J, Lai HH, Zou LB, Chen WB, Zhou XM, Lv DJ, Cen SR, Long ZN, *et al*: Exosomal PGAM1 promotes prostate cancer angiogenesis and metastasis by interacting with ACTG1. Cell Death Dis 14: 502, 2023.
53. Hu W, Li F, Liang Y, Liu S, Wang S, Shen C, Zhao Y, Wang H and Zhang Y: Glut3 overexpression improves environmental glucose uptake and antitumor efficacy of CAR-T cells in solid tumors. J Immunother Cancer 13: e010540, 2025.
54. Xu M, Zhong W, Yang C, Liu M, Yuan X, Lu T, Li D, Zhang G, Liu H, Zeng Y, *et al*: Tiliroside disrupted iron homeostasis and induced ferroptosis via directly targeting calpain-2 in pancreatic cancer cells. Phytomedicine 127: 155392, 2024.
55. Wu H, Yang J, Yang Z, Xiao Y, Liu R, Jia J, Zhang X, Zhang Y, Fu Z, Yao Z and Lv J: Targeting the BCKDK/BCLAF1/MYC/HK2 axis to alter aerobic glycolysis and overcome Trametinib resistance in lung cancer. Cell Death Differ 32: 2210-2224, 2025.
56. Wang L, Kong L, Zhang DQ, Ye L, Nao SC, Chan DS, Li X, Peng Y, Yang L and Wong CY: Inhibiting glycolysis and disrupting the mitochondrial HK2-VDAC1 Protein-protein interaction using a bifunctional Lonidamine-conjugated metal probe for combating Triple-negative breast cancer. J Am Chem Soc 147: 14824-14836, 2025.
57. Zhang W, Xia M, Li J, Liu G, Sun Y, Chen X and Zhong J: Warburg effect and lactylation in cancer: Mechanisms for chemoresistance. Mol Med 31: 146, 2025.
58. Bononi G, Masoni S, Di Bussolo V, Tuccinardi T, Granchi C and Minutolo F: Historical perspective of tumor glycolysis: A century with Otto Warburg. Semin Cancer Biol 86: 325-333, 2022.
59. Chen Y, Bei J, Liu M, Huang J, Xie L, Huang W, Cai M, Guo Y, Lin L and Zhu K: Sublethal heat stress-induced O-GlcNAcylation coordinates the Warburg effect to promote hepatocellular carcinoma recurrence and metastasis after thermal ablation. Cancer Lett 518: 23-34, 2021.
60. Guo Y, Li X, Sun X, Wang J, Yang X, Zhou X, Zhou X, Liu X, Liu W, Yuan J, *et al*: Combined aberrant expression of NDRG2 and LDHA predicts hepatocellular carcinoma prognosis and mediates the anti-tumor effect of gemcitabine. Int J Biol Sci 15: 1771-1786, 2019.
61. Yadav D, Yadav A, Bhattacharya S, Dagar A, Kumar V and Rani R: GLUT and HK: Two primary and essential key players in tumor glycolysis. Semin Cancer Biol 100: 17-27, 2024.
62. Gu J, Cao H, Chen X, Zhang XD, Thorne RF and Liu X: RNA m6A modifications regulate crosstalk between tumor metabolism and immunity. Wiley Interdiscip Rev RNA 15: e1829, 2024.
63. Li Y, He L, Wang Y, Tan Y and Zhang F: N6-methyladenosine methyltransferase KIAA1429 elevates colorectal cancer aerobic glycolysis via HK2-dependent manner. Bioengineered 13: 11923-11932, 2022.
64. Wang Q, Chen C, Ding Q, Zhao Y, Wang Z, Chen J, Jiang Z, Zhang Y, Xu G, Zhang J, *et al*: METTL3-mediated m6A modification of HDGF mRNA promotes gastric cancer progression and has prognostic significance. Gut 69: 1193-1205, 2020.
65. Yang N, Wang T, Li Q, Han F, Wang Z, Zhu R and Zhou J: HBXIP drives metabolic reprogramming in hepatocellular carcinoma cells via METTL3-mediated m6A modification of HIF-1α. J Cell Physiol 236: 3863-3880, 2021.
66. Peng H, Chen B, Wei W, Guo S, Han H, Yang C, Ma J, Wang L, Peng S, Kuang M and Lin S: N6-methyladenosine (m6A) in 18S rRNA promotes fatty acid metabolism and oncogenic transformation. Nat Metab 4: 1041-1054, 2022.
67. Rong B, Zhang Q, Wan J, Xing S, Dai R, Li Y, Cai J, Xie J, Song Y, Chen J, *et al*: Ribosome 18S m6A Methyltransferase METTL5 promotes translation initiation and breast cancer cell growth. Cell Rep 33: 108544, 2020.
68. Yang GJ, Tao F, Zhong HJ, Yang C and Chen J: Targeting PGAM1 in cancer: An emerging therapeutic opportunity. Eur J Med Chem 244: 114798, 2022.
69. Huang K, Liang Q, Zhou Y, Jiang LL, Gu WM, Luo MY, Tang YB, Wang Y, Lu W, Huang M, *et al*: A novel allosteric inhibitor of phosphoglycerate Mutase 1 suppresses growth and metastasis of non-small-cell lung cancer. Cell Metab 30: 1107-1119.e8, 2019.
70. Zhang D, Li J, Xu X, Wang X, Lou Y, Zhou X and Zhang K: CAF-derived GLUT1 and its role in modulating ovarian cancer progression: A multi-dimensional analysis of the tumor microenvironment. Commun Biol 8: 1020, 2025.
71. Luo J, Wang H, Wang L, Wang G, Yao Y, Xie K, Li X, Xu L, Shen Y and Ren B: lncRNA GAS6-AS1 inhibits progression and glucose metabolism reprogramming in LUAD via repressing E2F1-mediated transcription of GLUT1. Mol Ther Nucleic Acids 25: 11-24, 2021.
72. Li T, Xu D, Ruan Z, Zhou J, Sun W, Rao B and Xu H: Metabolism/Immunity Dual-Regulation thermogels potentiating immunotherapy of glioblastoma through Lactate-excretion inhibition and PD-1/PD-L1 blockade. Adv Sci (Weinh) 11: e2310163, 2024.
73. Kim JY, Hong N, Park S, Ham SW, Kim EJ, Kim SO, Jang J, Kim Y, Kim JK, Kim SC, *et al*: Jagged1 intracellular domain/SMAD3 complex transcriptionally regulates TWIST1 to drive glioma invasion. Cell Death Dis 14: 822, 2023.